Published in final edited form as:
Sci Signal. ; 6(303): ra101. doi:10.1126/scisignal.2004411.

Diacylglycerol Kinase ζ Limits the Generation of Natural Regulatory T Cells

Amanda M. Schmidt[1], **Tao Zou**[1], **Rohan P. Joshi**[2], **Theresa M. Leichner**[1], **Matthew A. Pimentel**[2], **Connie L. Sommers**[3], and **Taku Kambayashi**[1,†]

[1]Department of Pathology and Laboratory Medicine, Perelman School of Medicine at the University of Pennsylvania, Philadelphia, PA 10194, USA

[2]Abramson Family Cancer Research Institute, University of Pennsylvania, Philadelphia, PA 19104, USA

[3]Laboratory of Cellular and Molecular Biology, National Cancer Institute, National Institutes of Health, Bethesda, MD 20892, USA

Abstract

Natural regulatory T (nTreg) cells are important for maintaining tolerance to self and foreign antigens, and they are thought to develop from thymocytes that receive strong T cell receptor (TCR)-mediated signals in the thymus. TCR engagement leads to the activation of phospholipase C γ1, which generates the lipid second messenger diacylglycerol (DAG) from phosphatidylinositol-4,5-bisphosphate. Here, we used mice that lack the ζ isoform of DAG kinase (DGKζ), which metabolizes DAG to terminate its signaling, to enhance TCR-mediated signaling and identify critical signaling events in nTreg cell development. Loss of DGKζ resulted in increased numbers of thymic $CD25^+Foxp3^-CD4^+$ nTreg cell precursors and $Foxp3^+CD4^+$ nTreg cells in a cell-autonomous manner. DGKζ-deficient T cells exhibited increased nuclear translocation of the nuclear factor κB subunit c-Rel, as well as enhanced extracellular signal–regulated kinase (ERK) phosphorylation in response to TCR stimulation, suggesting that these downstream pathways may contribute to nTreg cell development. Indeed, reducing c-Rel abundance or blocking ERK phosphorylation abrogated the increased generation of nTreg cells by DGKζ-deficient thymocytes. The extent of ERK phosphorylation correlated with TCR-mediated acquisition of Foxp3 in immature thymocytes in vitro. Furthermore, the development of nTreg cells was augmented in mice in which ERK activation was selectively enhanced in T cells. Together, these data suggest that DGKζ regulates the development of nTreg cells by limiting the extent of activation of the ERK and c-Rel signaling pathways.

†Corresponding author. taku.kambayashi@uphs.upenn.edu.

Author contributions: A.M.S. and T.Z. conceived, designed, and performed experiments; A.M.S. wrote the manuscript; R.P.J., T.M.L., and M.A.P. performed experiments and provided stimulating discussion; C.L.S. provided key reagents; and T.K. conceived and supervised the work, designed experiments, and aided in writing of the manuscript.

Competing interests: The authors declare that they have no competing interests.

Introduction

Immune tolerance to self and foreign antigens must be actively maintained by $CD4^+Foxp3^+$ regulatory T (Treg) cells (1, 2). The importance of these cells has been described in various human and murine disorders in which a lack of Treg cells results in fatal autoimmune pathology because of unregulated activation of T cells (3-7). Treg cells also infiltrate tumors and block beneficial T cell–mediated anti-tumor responses (8). In addition to opposing immune responses to self, Treg cells also dampen excessive immune responses to foreign and commensal antigens that may otherwise lead to tissue damage (9-11). For example, depletion of Treg cells elicits inflammatory bowel disease that is caused by an unopposed immune response to commensal organisms in the gut (12). Thus, an understanding of the developmental requirements of these cells is paramount for devising effective therapeutic strategies in settings of autoimmunity, cancer, and infection.

Treg cells are defined by the presence of their lineage-determining transcription factor Foxp3, and they are divided into two subsets: natural Treg (nTreg) cells and inducible Treg (iTreg) cells. Whereas iTreg cells are generated from $Foxp3^-$ conventional T cells that acquire Foxp3 in the periphery (13), nTreg cells acquire Foxp3 during thymic development as the final result of a sophisticated and highly regulated maturation process (14). During T cell development in the thymus, survival signals generated through the recognition of self peptide–bound major histocompatibility complex (MHC) by the T cell receptor (TCR) stimulates the positive selection of CD4 CD8 double positive (DP) thymocytes. However, T cells bearing TCRs with excessive affinity for self peptide–bound MHC are purged through the process of negative selection. These developmental phases enable the selection of a highly diverse population of T cells that are not overtly self-reactive, but can still recognize foreign peptides presented by self MHC molecules. Although interaction with strong agonist peptides stimulates negative selection in many developing T cells, it can also induce the development of CD4 single positive (SP) thymocytes into nTreg cells (15). This phenomenon was demonstrated primarily through the use of TCR transgenic mouse models in which almost all T cells express a TCR of single specificity. Such studies have found that an unusually high percentage of T cells expressing a fixed TCR become Treg cells when their cognate antigen is present in the thymus during development (16-20). Additionally, when T cells express a TCR with an intrinsically lower affinity for this thymically expressed antigen, fewer Treg cells are generated, which suggests that strong TCR-mediated signals stimulate the development of nTreg cells (19, 21). However, the specific TCR-driven signaling events that induce the development of nTreg cells upon recognition of a TCR agonist have yet to be defined.

Engagement of the TCR on T cells leads to the formation of a multimolecular proximal signaling complex, which brings key signaling molecules in close proximity to each other and to the plasma membrane (22). One important event that results from the organization of this signaling complex is the activation and membrane localization of phospholipase C γ1 (PLC-γ1), which cleaves the plasma membrane–associated lipid molecule phosphatidylinositol-4,5-bisphosphate (PIP_2) to form the second messengers inositol-1,4,5-trisphosphate (IP_3) and diacylglycerol (DAG). IP_3 molecules initiate the release of Ca^{2+} from intracellular stores, whereas DAG promotes activation of the RAS guanine nucleotide–

releasing protein (Ras-GRP) and protein kinase C (PKC) signaling pathways. Activation of PLC-γ1, and the subsequent generation of IP_3 and DAG, represents a highly important step in TCR signal transduction, because a large array of gene expression outcomes important for T cell activation arise from this event (23).

Here, we evaluated the role of the ζ isoform of DAG kinase (DGKζ) in the development of nTreg cells. DGKζ metabolizes DAG into phosphatidic acid (PA), thereby terminating DAG-mediated signaling downstream of the TCR (24). Accordingly, T cells that lack DGKζ exhibit decreased conversion of DAG to PA upon TCR stimulation, which leads to the enhanced activation of TCR-stimulated T cells in DGKζ knockout (DGKζ$^{-/-}$) mice (24-27)). These observations prompted us to investigate Treg cell development in DGKζ$^{-/-}$mice to determine how it might be affected by the decreased conversion of DAG to PA. We demonstrated that a deficiency in DGKζ led to the increased production of nTreg cell precursors and nTreg cells in a cell-intrinsic manner through a mechanism that depended on extracellular signal–regulated kinase (ERK) and the nuclear factor κB (NF-κB) subunit c-Rel. These findings identify DGKζ as a critical molecule downstream of TCR signaling that regulates the development of nTreg cells.

Results

DGKζ-deficient thymocytes perceive enhanced signaling upon TCR engagement

Previous studies showed that the development of Treg cells results from strong signals received through the TCR during T cell maturation (16-20). To examine whether the selective enhancement of DAG-mediated signals is perceived by thymocytes as a strong TCR signal, we isolated thymocytes from DGKζ$^{-/-}$ mice and assessed them ex vivo for the abundance of Nur77 upon TCR stimulation. The abundance of Nur77 protein positively correlates with TCR signal strength (28-30). DGKζ$^{-/-}$ thymocytes stimulated through the TCR in the absence or presence of costimulation of CD28 exhibited a more rapid increase in Nur77 abundance than did wild-type thymocytes (Fig. 1A), which was true for both DP thymocytes and CD4 SP thymocytes. These data suggest that for a given stimulus, DGKζ$^{-/-}$ thymocytes perceive enhanced TCR signals compared to wild-type thymocytes.

The percentages and numbers of thymic and peripheral Treg cells in DGKζ$^{-/-}$ mice are increased compared to those in wild-type mice

We next examined the numbers and percentages of Treg cells in DGKζ$^{-/-}$ mice. Compared to those of age-matched wild-type mice, the percentages of Treg cells within all CD4$^+$ SP T cells and the absolute numbers of Treg cells were statistically significantly increased in the thymus and spleen of DGKζ$^{-/-}$ mice (Fig. 1, B and C). DGKζ$^{-/-}$ mice did not exhibit a substantial reduction in the absolute numbers of Foxp3$^-$ CD4 SP thymocytes or of Foxp3$^-$CD4$^+$ splenic T cells (Fig. 1C), which suggested that the enhanced percentages of Treg cells were not a result of decreased numbers of Foxp3$^-$CD4$^+$ T cells. In addition to Foxp3$^+$CD4$^+$ Treg cells in the thymus, DGKζ$^{-/-}$ mice also had increased percentages of CD25$^+$Foxp3$^-$ CD4 SP thymocytes, a population that is highly enriched for nTreg cell precursors (Fig. 1D) (31). Similar to adult mice, 3-week-old DGKζ$^{-/-}$ mice had increased percentages and numbers of Treg cells in the thymus and spleen compared to those of age-

matched wild-type mice (fig. S1, A and B). Moreover, DGKζ$^{-/-}$ mice exhibited increased percentages of Foxp3^{+} cells within the fraction of CD4 SP T cells that had not yet decreased the abundance of heat stable antigen (HSA), a protein present on the cell surface of developing T cells (Fig. 1E) (32). Together, these data suggest that a deficiency in DGKζ leads to the increased generation of nTreg cell precursors and nTreg cells in the thymus.

To ensure that the CD4^{+}Foxp3^{+} T cells generated in DGKζ$^{-/-}$ mice were bona fide Treg cells with suppressive function, we compared the phenotypes and functions of Treg cells in wild-type and DGKζ$^{-/-}$ mice. We found that the amounts of CD25, Foxp3, and the glucocorticoid-induced tumor necrosis factor receptor (TNFR) family related gene (GITR), a molecule constitutively present on the surface of Treg cells, were similar between wild-type and DGKζ$^{-/-}$ Treg cells (fig. S2). We then crossed DGKζ$^{-/-}$ mice to Foxp3 green fluorescent protein (GFP) reporter mice, and then compared the suppressive abilities of sorted DGKζ$^{-/-}$ Treg cells with those of wild-type Treg cells in vitro. DGKζ$^{-/-}$ Treg cells suppressed the TCR-stimulated division of CD4^{+} T cells at least as well as did wild-type Treg cells, suggesting that DGKζ$^{-/-}$ Treg cells are bona fide Treg cells with normal function (Fig. 1F).

Loss of DGKζ enhances the generation of Treg cell precursors and Treg cells in a cell-autonomous manner

Because both the development and peripheral homeostasis of thymic Treg cells are dependent on extrinsic factors such as interleukin-2 (IL-2) (1, 33), we next tested whether the enhanced generation of Treg cells in DGKζ$^{-/-}$ mice was a result of a cell-intrinsic or a cell-extrinsic effect. To this end, we generated competitive bone marrow chimeric mice with bone marrow cells from DGKζ$^{-/-}$ or wild-type mice mixed with competitor bone marrow cells from congenically disparate wild-type mice. We then analyzed the development of thymic Treg cells and CD25^{+}Foxp3^{-}CD4 SP nTreg cell precursors from the wild-type or DGKζ$^{-/-}$ bone marrow cells, as well as from their respective competitor wild-type bone marrow cells. We found that there was a statistically significant increase in the percentages of thymic Treg cells and Treg cell precursors derived from DGKζ$^{-/-}$ bone marrow cells compared to those that originated from wild-type bone marrow cells (Fig. 2A). In contrast, we observed a slight, but statistically significant, decrease in the number of wild-type competitor Treg cells in the DGKζ$^{-/-}$ chimeras compared to that in the wild-type bone marrow chimeras (Fig. 2A). This decrease was to be expected because of the increased occupancy of the Treg cell niche by the DGKζ$^{-/-}$ Treg cells. DGKζ$^{-/-}$ bone marrow cells also gave rise to an increased percentage of Treg cells within the splenic T cell compartment (Fig. 2B).

To further investigate whether developing DGKζ$^{-/-}$ thymocytes had an increased intrinsic ability to become Treg cells upon TCR stimulation, we used an in vitro Treg cell differentiation assay that was free of antigen-presenting cells (APCs). A small, but reproducible, percentage of sorted immature CD4 SP thymocytes (Foxp3^{-}CD25^{-}CD44^{lo}CD69^{hi}) were previously shown to express Foxp3 when provided with only a TCR stimulus in the presence of IL-2 (34). This method enabled us to completely remove additional costimulatory or environmental cues that might contribute to

the enhanced percentage of Foxp3$^+$ CD4 SP thymocytes in DGKζ$^{-/-}$ mice. After a 72-hour stimulation with anti-CD3 antibody (to stimulate the TCR) and IL-2, sorted immature CD4 SP T cells from the thymi of DGKζ$^{-/-}$ mice consistently produced statistically significantly more Foxp3$^+$ T cells than did their wild-type counterparts (Fig. 2C). This difference in the percentage of Foxp3$^+$ thymocytes was not a result of differences in the proliferation or viability of the cultured wild-type and DGKζ$^{-/-}$ thymocytes (fig. S3, A and B). These data suggest that the increased development of Treg cells exhibited by DGKζ$^{-/-}$ CD4 SP T cells occurs in a T cell– intrinsic manner.

DGKζ$^{-/-}$ thymocytes require CD28 costimulation for the enhanced development of Treg cells

Deficiency in one or more isoforms of DGK compensates for certain costimulation requirements in T cell activation and division (24, 26). Because developing thymocytes require CD28 costimulation to develop into Treg cells (35-38), we wondered whether a deficiency in DGKζ could compensate for this necessity and restore the developmental defect in nTreg cells in CD28$^{-/-}$ mice. To test this notion, we crossed DGKζ$^{-/-}$ mice to CD28$^{-/-}$ mice to generate DGKζ$^{-/-}$ CD28$^{-/-}$ mice. To avoid potential cell-extrinsic factors, we assessed Treg cell development in a competitive bone marrow chimeric setting with wild-type, DGKζ$^{-/-}$, CD28$^{-/-}$, or DGKζ$^{-/-}$CD28$^{-/-}$ bone marrow cells mixed with competitor bone marrow cells from congenically disparate wild-type mice. As expected, nTreg cell development from DGKζ$^{-/-}$ bone marrow cells was enhanced compared to that of wild-type bone marrow cells (Fig. 3, A to C). However, Treg cell development from DGKζ$^{-/-}$CD28$^{-/-}$ bone marrow, although increased in comparison to that from CD28$^{-/-}$ bone marrow, was decreased compared to that from wild-type bone marrow in the thymus and spleen (Fig. 3, A to C). Therefore, DGKζ deficiency did not simply replace the need for costimulation in the development of nTreg cells.

c-Rel–mediated signals are required for the enhanced development of nTreg cells in DGKζ$^{-/-}$ mice

We next sought to determine the specific downstream signals regulated by DGKζ that might be involved in the enhanced generation of nTreg cells. We first assessed the NF-κB pathway, in particular the NF-κB subunit c-Rel, because numerous studies have described an essential role for c-Rel in the development of Treg cells (35, 39-44). Activation of NF-κB family transcription factors requires phosphorylation of the inhibitory molecule inhibitor of κB α (IκBα), leading to its proteasomal degradation, which enables c-Rel and other sequestered NF-κB family members to shuttle to the nucleus and activate gene expression (45). Thus, we examined the phosphorylation and degradation of IκBα and the nuclear translocation of c-Rel in CD4$^+$ T cells from wild-type and DGKζ$^{-/-}$ mice. Upon TCR stimulation, both the phosphorylation and degradation of IκBα were enhanced in DGKζ$^{-/-}$ T cells compared to in wild-type CD4$^+$ T cells (Fig. 4A). Moreover, the nuclear translocation of c-Rel was augmented in cells lacking DGKζ compared to that in wild-type cells (Fig. 4A). These data suggest that DGKζ$^{-/-}$ mice exhibit enhanced NF-κB signaling, including that of c-Rel.

To test whether c-Rel was involved in the enhanced development of nTreg cells in DGKζ$^{-/-}$ mice, we crossed these mice with c-Rel$^{-/-}$ mice to generate DGKζ$^{-/-}$c-Rel$^{-/-}$ mice. Because nTreg development is markedly reduced in c-Rel$^{-/-}$ mice (39-41) and the nuclear translocation of c-Rel is enhanced in DGKζ$^{-/-}$ mice compared to that in wild-type mice, we predicted that the absence of DGKζ would not increase the extent of Treg cell generation in the absence of c-Rel. As described earlier, we assessed Treg cell development in a competitive bone marrow chimeric setting with wild-type, DGKζ$^{-/-}$, c-Rel$^{-/-}$, or DGKζ$^{-/-}$c-Rel$^{-/-}$ bone marrow cells mixed with competitor bone marrow cells from congenically different wild-type mice. As expected, Treg cell development from DGKζ$^{-/-}$ bone marrow cells was enhanced compared to that from wild-type bone marrow cells (Fig. 4, B to D). In contrast, the extent of Treg cell development from DGKζ$^{-/-}$c-Rel$^{-/-}$ bone marrow cells was similar to that from c-Rel$^{-/-}$ bone marrow cells, which was markedly and statistically significantly less than that from wild-type bone marrow cells in the thymus and spleen (Fig. 4, B to D). These data suggest that signals through c-Rel are required for appreciable Treg cell development, even in the absence of DGKζ.

We next tested whether Treg cell development in the context of DGKζ deficiency was attenuated in mice with reduced amounts of c-Rel. To this end, we additionally created competitive bone marrow chimeras with bone marrow cells from c-Rel$^{+/-}$ mice or DGKζ$^{-/-}$c-Rel$^{+/-}$ mice mixed with competitor bone marrow cells from congenically disparate wild-type mice. The extent of Treg cell generation from DGKζ$^{-/-}$c-Rel$^{+/-}$ bone marrow was similar to that from wild-type bone marrow, which was statistically significantly reduced compared to that from DGKζ$^{-/-}$ bone marrow (Fig. 4, B to D). Thus, in the absence of DGKζ, the augmented generation of Treg cells was dependent on the amount of c-Rel available, with both alleles of *Rel* required for maximal Treg cell development.

The extent of TCR-dependent ERK phosphorylation directly correlates with the amount of Foxp3$^+$ cell generation by thymocytes from wild-type and DGKζ$^{-/-}$ mice

Another major downstream signaling pathway regulated by DGKζ involves activation of ERK (46). Consistent with previous reports (24, 25), we found that DGKζ$^{-/-}$ CD4$^+$ T cells exhibited increased phosphorylation (and activation) of mitogen-activated and extracellular signal– regulated kinase (MEK) and ERK compared to that in wild-type CD4$^+$ T cells upon TCR stimulation (Fig. 5, A and B). To investigate whether the enhanced ERK activation in DGKζ$^{-/-}$ cells had an effect on the development of Treg cells, we performed an in vitro Treg cell development assay in the presence of the MEK1/2 inhibitor U0126 (47). ERK phosphorylation, but not upstream signaling events [for example, phosphorylation of the adaptor protein SLP-76 [Src homology 2 (SH2) domain–containing leukocyte phosphoprotein of 76 kD] was completely inhibited in both wild-type and DGKζ$^{-/-}$ CD4$^+$ T cells treated with 30 μM U0126 (Fig. 5B). The same concentration of U0126 prevented the generation of Foxp3$^+$ cells by both wild-type and DGKζ$^{-/-}$ immature CD4 SP thymocytes in vitro (Fig. 5C). These data suggest that ERK phosphorylation is required for the generation of Foxp3$^+$ cells by immature CD4 SP thymocytes.

Because IL-2 also leads to ERK activation (48), we wondered whether IL-2–dependent ERK signaling was required to generate Foxp3$^+$ cells. To this end, we performed a two-step Treg

cell differentiation assay in vitro in which the TCR stimulus and IL-2 were provided separately and sequentially. Immature thymocytes were stimulated through their TCR in the absence of IL-2 for 20 hours and re-sorted to obtain $CD25^+$ thymocytes, which were then cultured for an additional 60 hours in the presence of IL-2 alone. Approximately 25% of $CD25^+$ thymocytes gave rise to $Foxp3^+$ cells upon addition of exogenous IL-2, even in the presence of U0126 (Fig. 5D). These data suggest that ERK activation is dispensable for IL-2–dependent $Foxp3^+$ cell generation by $CD25^+$ CD4 SP thymocytes.

Next, to correlate the extent of ERK phosphorylation to the generation of $Foxp3^+$ cells, we titrated the concentration of U0126 used in the experiments. As expected because of the enhanced activation of MEK observed in DGK$\zeta^{-/-}$ cells (Fig. 5A), a greater concentration of U0126 was required to inhibit ERK phosphorylation in DGK$\zeta^{-/-}$ $CD4^+$ T cells than was required for wild-type $CD4^+$ T cells (Fig. 5E). Moreover, $Foxp3^+$ cell generation was inhibited by U0126 in a dose-dependent manner in both DGK$\zeta^{-/-}$ and wild-type immature CD4 SP thymocytes (Fig. 5F). We next quantified the amount of phosphorylated ERK (pERK) at various U0126 concentrations, and plotted these against the percentage of $Foxp3^+$ cells in the nTreg cell development assays in which the same concentration of U0126 was used. When normalized to pERK amounts, the percentage of CD4 SP thymocytes that were $Foxp3^+$ was no longer increased in TCR-stimulated DGK$\zeta^{-/-}$ immature CD4 SP thymocytes compared to that in wild-type cells (Fig. 5G). Additionally, there was a linear correlation between pERK abundance and the percentage of $Foxp3^+$ cells, which suggested that TCR-dependent ERK activation promotes $Foxp3^+$ cell generation from developing $CD4^+$ SP thymocytes. However, at increased amounts of pERK, the generation of $Foxp3^+$ cells reached an upper limit such that beyond a certain amount, increased pERK abundance was no longer associated with enhanced percentages of $Foxp3^+$ cells (Fig. 5G). These findings suggest that the increased abundance of pERK seen in the absence of DGKζ promotes Foxp3 production in immature thymocytes in a dose-dependent manner.

Enhanced TCR-mediated activation of ERK promotes Treg cell development in vivo

To further test the role of ERK signaling in the development of nTreg cells, we assessed Treg cell development in transgenic mice bearing the gain-of-function ERK mutation known as sevenmaker (ERK^{SEM}). The sevenmaker mutation renders pERK less sensitive to deactivation by phosphatases, which leads to prolonged activation of ERK (49). Compared to wild-type mice, ERK^{SEM} mice exhibited a substantially increased percentage of Treg cells within the $CD4^+$ T cell population in both the thymus and the spleen (Fig. 6A). As was observed for DGK$\zeta^{-/-}$ mice, the absolute numbers of Treg cells were also increased in both the thymus and the spleen of ERK^{SEM} mice compared to those of wild-type mice, whereas the absolute numbers of $Foxp3^-CD4^+$ T cells remained unchanged (Fig 6B). Additionally, there was a statistically significantly increase in the percentage of $CD25^+$ CD4 SP thymocytes (which are enriched in Treg cell precursors) in ERK^{SEM} mice compared to that in wild-type mice (Fig. 6C). Together, our in vitro and in vivo findings support a positive role for ERK in the generation of nTreg cells, and suggest that the enhanced ERK activation intrinsic to DGK$\zeta^{-/-}$ T cells contributes to the increased nTreg cell development observed in DGK$\zeta^{-/-}$ mice.

The NF-κB and ERK signaling pathways are not interdependently activated upon TCR stimulation of DGKζ$^{-/-}$ T cells

Given that both the NF-κB and ERK signaling pathways downstream of the TCR contributed to the increased development of Treg cells in DGKζ$^{-/-}$ mice, it was possible that the two pathways were interdependent. To test this, we performed biochemical analyses of the activation of NF-κB signaling in DGKζ$^{-/-}$ CD4^{+} T cells that were stimulated in the presence of a large concentration of U0126. Both the phosphorylation and degradation of IκBα were unaffected in these cells, despite the complete abrogation of ERK phosphorylation by U0126 (fig. S4A). Next, we assessed TCR-mediated ERK phosphorylation in c-Rel$^{-/-}$ CD4^{+} T cells. Western blotting analysis revealed that TCR-dependent ERK phosphorylation in c-Rel$^{-/-}$ CD4^{+} T cells was similar to, if not greater than that observed in wild-type CD4^{+} T cells (fig. S4B). These findings suggest that the ERK and NF-κB signaling pathways do not substantially influence each other in CD4^{+} T cells stimulated through the TCR. These data suggest that the c-Rel and ERK pathways are likely two independent signaling pathways downstream of TCR-dependent DAG activation that contribute to the enhanced development of Treg cells in DGKζ$^{-/-}$ mice.

Discussion

Here, we used mice lacking DGKζ to identify signaling pathways downstream of the TCR that affected the development of nTreg cells. We found that TCR-stimulated DGKζ$^{-/-}$ thymocytes more rapidly increased the abundance of Nur77 than did wild-type thymocytes, suggesting that stronger signals are perceived by thymocytes in the absence of DGKζ. Consistent with the notion that strong TCR signaling leads to the development of nTreg cells in the thymus, loss of DGKζ promoted Treg cell development in a cell-intrinsic manner. The absence of DGKζ resulted in increased activation of the NF-κB (including c-Rel) and ERK signaling pathways, each of which contributed to the enhanced development of Treg cells in DGKζ$^{-/-}$ mice. Together, our data suggest that DGKζ inhibits nTreg cell development by attenuating signals that lead to the activation of c-Rel and ERK (Fig. 7).

Loss of DGKζ appears to promote Treg cell development at least in part by enhancing the generation of Treg cell precursors. Compared to wild-type mice, DGKζ$^{-/-}$ mice and DGKζ$^{-/-}$ bone marrow chimeric mice exhibited increased percentages of CD25^{+}Foxp3^{-} CD4 SP thymocytes in the thymus. The development of Treg cells from the CD4 SP thymocyte stage is thought to occur in two separate steps (31, 36). First, thymic CD4 SP T cells increase their abundance of the high-affinity IL-2 receptor (IL-2R) subunit CD25 in a TCR-dependent manner to generate CD25^{+}Foxp3^{-} CD4 SP T cells, which are highly enriched in Treg cell progenitors (31, 36, 50). The second step, which involves the induction of *Foxp3* expression by CD25^{+}Foxp3^{-} CD4 SP T cells, is dependent on IL-2, but not on TCR stimulation (31, 36). Thus, it is likely that enhanced TCR-mediated signaling in the setting of DGKζ deficiency would exert its effect during the TCR-dependent phase, leading to the cell-surface expression of CD25 and increased generation of Treg cell progenitors. Indeed, c-Rel, NF-κB1, and activating protein 1 (AP-1, a key transcription factor activated by ERK) can bind within the promoter and enhancer regions of *Il2ra*, the gene encoding CD25, and serve to enhance *IL2ra* expression upon T cell stimulation (51-54). In support of

this notion, we observed that the enhancement of TCR-mediated ERK activation in vivo by itself caused an increase in the numbers of Treg cells and Treg cell progenitors in ERK^{SEM} mice similar to that observed in DGKζ$^{-/-}$ mice. Thus, these data suggest that increased TCR-dependent cell-surface expression of CD25 by immature thymocytes in the context of a lack of DGKζ contributes to the augmented generation of Treg cells.

In addition to promoting the generation of Treg cell precursors, the absence of DGKζ might enhance the transition of Treg cell precursors to Treg cells by promoting the nuclear translocation of c-Rel. Not all $CD25^{+}Foxp3^{-}$ CD4 SP thymocytes convert to $Foxp3^{+}CD4^{+}$ T cells upon stimulation with IL-2 (31). Thus, although the generation of Treg cells from Treg cell precursors is TCR-independent, transcriptional programs activated at the TCR-dependent stage might determine the likelihood that IL-2 can convert Treg cell precursors into Treg cells. Consistent with this notion, c-Rel is required for the initial TCR-mediated opening of the *Foxp3* locus by binding to a conserved non-coding DNA sequence element (CNS3) (44). Furthermore, c-Rel cooperates with other transcription factors to form an enhanceosome that binds to the *Foxp3* promoter to drive gene expression (43). Accordingly, c-Rel$^{-/-}$ mice exhibit a severe deficiency in Treg cells (35, 39-41), whereas mice bearing a constitutively active form of inhibitor of IκB kinase β (IKKβ) display increased numbers of Treg cells (42). Our data demonstrate that $CD4^{+}$ T cells from DGKζ$^{-/-}$ mice display increased NF-κB signaling, including enhanced nuclear translocation of c-Rel, suggesting that c-Rel translocation is one likely mechanism contributing to augmented nTreg cell development in these mice. Indeed, DGKζ$^{-/-}$c-Rel$^{-/-}$ mice and c-Rel$^{-/-}$ mice exhibited a similar and marked reduction in nTreg cell generation. Additionally, the development of nTreg cells in the absence of DGKζ was normalized similar to that in wild-type mice when only one allele of *c-Rel* was present. Thus, the increased generation of nTreg cells in DGKζ$^{-/-}$ mice was dependent on the number of *Rel* alleles, supporting the notion that DAG-mediated signals contribute to the generation of nTreg cells by activation of c-Rel.

In addition to exhibiting enhanced NF-κB signaling compared to wild-type $CD4^{+}$ T cells, DGKζ$^{-/-}$ $CD4^{+}$ T cells showed markedly augmented ERK activation. The addition of a MEK1/2 inhibitor blocked ERK phosphorylation and Foxp3 production by immature thymocytes in a dose-dependent manner. Furthermore, a linear and positive correlation was established between the degree of ERK phosphorylation and the percentage of immature thymocytes expressing Foxp3. Together with the increase in Treg cell generation that we observed in ERK^{SEM} mice, these data suggest that the enhancement of ERK activation is another mechanism that promotes nTreg cell development in DGKζ$^{-/-}$ mice. How ERK promotes the generation of nTreg cells is unclear. As suggested earlier, ERK activation may increase the number of Treg cell precursors by promoting the cell-surface expression of CD25 on CD4 SP thymocytes through the activation of AP-1 family transcription factors (51). Both TCR-mediated DAG production and IL-2R signaling lead to ERK activation; however, we found that ERK activation was dispensable for Foxp3 production in thymocytes that already had increased CD25 abundance. Still, it is possible that the AP-1 transcription factors activated during the initial TCR stimulus promoted *Foxp3* expression during Treg cell development. Several AP-1–binding sites are present in the *Foxp3* promoter, and reporter-based assays have shown that these sites are necessary for efficient

Foxp3 induction in peripheral human T cells (55). In addition to AP-1, ERK may promote *Foxp3* expression by phosphorylating the transcription factor Runx1, which enables the interaction of Runx1 with its binding partners and enhances its transcriptional activity (56, 57). Runx1 and its transcriptional coactivator Cbf-β associate with Foxp3 to form a complex that binds to the CNS2 region of the *Foxp3* locus, which is required for the stable expression of *Foxp3* in dividing nTreg cells (44, 58, 59). Therefore, TCR-mediated activation of ERK can act at multiple developmental steps leading to the generation of nTreg cells.

During our analyses comparing quantitative ERK phosphorylation versus *Foxp3* expression (Fig. 5G), we found that the y-intercepts of the lines were substantially different between wild-type and DGKζ$^{-/-}$ thymocytes, such that the line corresponding to the DGKζ$^{-/-}$ cells was shifted to the right of that corresponding to the wild-type cells. These data suggest that, for a given amount of pERK, immature DGKζ$^{-/-}$ T cells are less likely to give rise to Treg cells than are their wild-type counterparts. This finding suggests the presence of DGKζ-regulated signaling pathways that antagonize *Foxp3* expression. For example, DGKζ inhibits the DAG-mediated activation of Ras-GRP that leads to activation of the Akt–mammalian target of rapamycin (mTOR) pathway (60). Consistent with this finding, TCR-mediated phosphorylation of Akt and the mTOR pathway component S6 is markedly enhanced in DGKζ$^{-/-}$ CD4^{+} T cells compared to that in wild-type CD4+ T cells (27). Numerous studies have demonstrated that the Akt pathway inhibits *Foxp3* expression both in developing thymocytes and in peripheral CD4^{+} T cells (61, 62). Thus, DGKζ may concurrently regulate signaling pathways that both promote and inhibit the development of nTreg cells, with the overall balance biased towards increased nTreg cell generation. The inhibition of the positive regulator (ERK) by the MEK1/2 inhibitor might have unmasked the negative regulatory pathway (Akt). Unfortunately, the toxicity of Akt inhibitors has precluded us from performing experiments to compare how concurrent inhibition of Akt and ERK alters Treg cell generation by wild-type and DGKζ$^{-/-}$ thymocytes.

In addition to DGKζ, another isoform of DGK, DGKα, is also found in T cells. Like DGKζ, DGKα phosphorylates DAG to convert it to PA and terminates DAG-mediated signaling (63). Despite DGKα being three-fold more abundant than DGKζ in T cells, mice lacking DGKα do not exhibit enhanced nTreg cell generation (27). This lack of enhancement nTreg cell generation correlates with the reduced ability of DGKα$^{-/-}$ T cells to phosphorylate ERK (27), highlighting the importance of ERK activation in enhancing Treg cell generation.

Costimulatory signals from CD28 also are critical in the generation of nTreg cells (35-38). CD28 activation is important for the recruitment of PKCθ to the immunological synapse upon TCR stimulation, which enables the downstream NF-κB pathway to be fully activated (64, 65). Because DAG additionally recruits PKCθ to the immunological synapse (66), TCR-dependent DAG signals intersect with the CD28 signaling pathway at this step. CD28 costimulation is also thought to increase the hydrolysis of PIP_2, leading to the enhanced accumulation of DAG molecules simultaneous to TCR engagement (26). Thus, it is likely that the increased accumulation of DAG that occurs in DGKζ$^{-/-}$ T cells might either be perceived as or may contribute to CD28 costimulation. Indeed, T cells from DGKζ$^{-/-}$ mice, but not wild-type mice, proliferate in the absence of CD28 costimulation (26). Moreover, we found that the severe developmental defect in Treg cells normally observed in CD28$^{-/-}$ mice

was partially rescued when CD28$^{-/-}$ mice were crossed to DGKζ$^{-/-}$ mice. Although the extent of this rescue was modest, these data suggest that the TCR and co-stimulatory signals at least in part converge upon the DAG signaling pathway to stimulate efficient development of Treg cells. This could enable developing DGKζ$^{-/-}$ T cells to generate enhanced output from a given TCR and costimulatory signal, leading to increased nTreg cell development.

The notion that strong TCR-dependent signals drive the thymic development of Treg cells is supported by several mouse models, most of which assess Treg cell development under circumstances of TCR restriction or provision of transgenically expressed self-antigen within the thymus (16-21). Although such models have been highly informative, it has been unclear which TCR signals influence the development of Treg cells in the unrestricted TCR setting where a full repertoire of TCR specificities exist. Our study demonstrated that enhanced TCR signaling caused by the absence of DGKζ led to an increase in the percentage of Treg cells in the setting of a full TCR repertoire. . Such a finding might be unexpected, because one might predict that T cell subset niches are fixed and that T cells would adjust their signals accordingly to fill these niches by selecting lower affinity TCRs in DGKζ$^{-/-}$ mice. In other words, T cells that would normally fail to undergo positive selection would now be positively selected, and cells that would otherwise enter into the population (or pool) of conventional T cells (Tconv) would instead become Treg cells or would be negatively selected in DGKζ$^{-/-}$ mice. However, the increased numbers of Treg cells that we observed in DGKζ$^{-/-}$ mice suggests that the Treg niche is expandable and that it may be augmented by generating more Treg cell precursors and Treg cells through the enhancement of TCR signaling. Studies performed by tracking the development of T cells bearing a fixed TCR β chain in the presence of transgenically expressed self-antigen have shown that the responsiveness of the TCR to self-antigen in vitro can be directly correlated with the frequency and absolute number of Treg cells produced in vivo (21). These findings and ours suggest that increased TCR affinity can effectively stimulate more developing T cells to become Treg cells.

Here, we demonstrated that the selective enhancement of TCR-dependent, DAG-mediated signals by loss of DGKζ stimulated the robust activation of c-Rel and ERK signaling, both of which promoted the generation of nTreg cells from developing thymocytes (Fig. 7). Our data support the role of strong TCR signals in directing developing T cells into the nTreg cell fate, and identify DGKζ as a key signaling molecule regulating this process. Manipulation of these signaling pathways might be beneficial in therapeutically enhancing the generation of Treg cells in the thymus.

Materials and Methods

Mice

C57BL/6, B6.SJL (CD45.1^{+}), B6.PL (CD90.1^{+}), B6 Foxp3.GFP reporter mice, and B6 CD28$^{-/-}$ mice were purchased from The Jackson Laboratory. DGKζ$^{-/-}$ mice that were backcrossed seven times to C57BL/6 mice were a gift of G. Koretzky and X. P. Zhong (24). c-Rel$^{-/-}$ mice were obtained from Dr. H.-C. Liou at Cornell University (67). ERK^{SEM} mice were provided by Dr. Stephen Hedrick (49). DGKζ$^{-/-}$CD28$^{-/-}$ mice were generated by crossing DGKζ$^{-/-}$ mice with CD28$^{-/-}$ mice. DGKζ$^{-/-}$c-Rel$^{-/-}$ mice and DGKζ$^{-/-}$cRel$^{+/-}$

mice were generated by crossing DGKζ$^{-/-}$ mice with c-Rel$^{-/-}$ mice. Unless otherwise specified, all mice were 6 to 16 weeks of age at the time of use, and were housed in pathogen-free conditions and treated in strict compliance with the Institutional Animal Care and Use Committee regulations of the University of Pennsylvania.

Reagents and antibodies

U0126 was purchased from Cell Signaling Technologies. All other chemicals were purchased from Sigma-Aldrich, unless otherwise specified. Streptavidin and LIVE/DEAD Fixable Dead Cell stain were purchased from Molecular Probes, Invitrogen. Anti-CD4 (RM4-5), anti-CD25 (PC61), anti-CD90.1 (OX-7), anti-CD8α (53-6.7), anti-SLP-76 pY128 (J141-668.36.58), anti-CD3 (2C11), and anti-CD28 (37.51) antibodies were purchased from BD Pharmingen; anti-CD45.2 (104), anti-CD45.1 (A20), anti-CD4 (GK1.5), anti-CD3 (2C11), anti-CD28 (37.51), and anti-CD24 (M1/69) antibodies were from Biolegend; anti-Nur77 (12.14), anti-CD44 (IM7), anti-CD69 (H1.2F3), anti-Foxp3 (FJK-16s), and anti-GITR (DTA-1) antibodies were from eBioscience; anti-PLC-γ1 (2822), anti-p44/42 MAPK (3A7), anti-phospho-p44/42 MAPK (9101), anti-IκBα (L35A5), anti-pIκBα (14D4), anti-pMEK (41G9), anti-β-tubulin (9F3), and anti-histone H3 (9715) antibodies were purchased from Cell Signaling Technologies; horseradish peroxidase (HRP)-conjugated goat anti-rabbit immunoglobulin G (IgG) and goat anti-mouse IgG-HRP were from Bio-Rad; and goat anti-mouse IgG 680RD and goat anti-rabbit IgG 800CW were from LI-COR Biosciences.

Flow cytometry, cell sorting, and data analysis

For flow cytometric analyses, cells were stained with antibodies against cell-surface antigens at 4°C for 20 min in phosphate-buffered saline (PBS). Intracellular Nur77 and Foxp3 staining was performed with the Foxp3 Staining Set (eBioscience) according to the manufacturer's protocol. Flow cytometry was performed with an LSR II or FACSCanto flow cytometer (BD Biosciences). For cell sorting, T cells were purified with either CD4 or CD90.2 magnetic beads with MACS columns (Miltenyi Biotec) according to the manufacturer's protocol before undergoing cell-surface staining. FACS (sorting) was performed with a FACSAria cell sorter (BD Biosciences). FACS-sorted populations were typically of 96 to 99% purity. Data were analyzed with FlowJo software (TreeStar). Cell division data from analysis of the dilution of carboxyfluorescein succinimidyl ester (CFSE) in Treg cells, gated on live CD4^{+}Foxp3^{+} cells, were transformed into “Division Index” data with the “Proliferation” function of FlowJo software. The “Division Index” measures the average number of divisions per cell.

Measuring Nur77 protein in thymocytes

Tissue culture plates were coated with anti-CD3 antibody (50 μg/ml) and anti-CD28 antibody (50 μg/ml) or with anti-CD3 antibody alone (25 μg/ml) for 3 hours at 37°C. Coated plates were washed, and freshly isolated thymocytes were added to wells in T cell medium [RPMI 1640 (Mediatech) with 10% fetal bovine serum (FBS, Atlanta Biologicals), penicillin (100 U/ml), streptomycin (100 μg/ml), 3 mM L-glutamine, 1% sodium pyruvate (Mediatech), 10 mM Hepes, 1% NEAA (Invitrogen), and 10 μM 2-ME (Bio-Rad)]. After incubation at 37°C for the times indicated in the figure legends, CD4^{+} cells were analyzed for the presence of intracellular Nur77 by flow cytometry.

In vitro Treg differentiation assays

$CD8^+$ cells were depleted from freshly isolated thymocytes by MACS beads, which was followed by FACS-based sorting of immature thymocytes (characterized as: $CD4^+CD44^{lo}CD69^+CD25^-Foxp3^-$). 5×10^5 immature thymocytes were cultured in tissue culture plates coated with anti-CD3 antibody (2 μg/ml) in the presence of recombinant human IL-2 (100 U/ml, Peprotech) for 20 or 72 hours. The 20-hour time point was chosen to avoid a two-fold increase in cellular toxicity that was observed for both wild-type and $DGK\zeta^{-/-}$ thymocytes after 72 hours in the presence of 30 μM U0126 (a MEK1/2 inhibitor). Such toxicity was not observed at lower concentrations of U1026. For the 20-hour time point, the culture plates were additionally coated with anti-CD28 antibody (2 μg/ml) to expedite *Foxp3* induction within the shorter time period. In some experiments, immobilized anti-CD3 antibody was provided alone for the first 20 hours of culture, $CD4^+CD25^+$ cells were then resorted by FACS, and these cells were cultured with soluble IL-2 alone for an additional 60 hours. In experiments involving MEK1/2 inhibition, cells were pretreated for one hour at 37°C with U0126 at various concentrations or with DMSO as a control, which was maintained throughout the assay. Cultured cells were analyzed for viability and for CD4, FoxP3, and CD25 abundance by flow cytometry.

Treg cell suppression assays

MACS-enriched $CD90.2^+$ T cells were sorted by FACS for $CD4^+Foxp3^+$ Treg cells from either wild-type or $DGK\zeta^{-/-}$ Foxp3.GFP reporter mice ($CD45.2^+$) or were sorted by FACS for $CD4^+Foxp3^-$ conventional T cells (Tconvs) from wild-type B6.SJL Foxp3.GFP reporter mice ($CD45.1^+$). The Tconvs were labeled with carboxyfluorescein succinimidyl ester (CFSE) and cultured at various ratios with Treg cells in the presence of irradiated, T cell-depleted $CD45.2^+$ feeder cells and soluble anti-CD3 antibody (1 μg/ml). CFSE labeling was performed by resuspending the cells with PBS containing CFSE (5 mM) at 37°C followed by continuous shaking for 9 min. The reaction was then immediately quenched with 100% FBS, and the cells were washed before being cultured. The extent of CFSE dilution in Tconvs ($CD4^+CD45.1^+$) was assessed by flow cytometry after 4 days in culture.

Generation of mixed bone marrow chimeric mice

Donor bone marrow cells were depleted of T cells by CD4 and CD8 magnetic bead depletion (Miltenyi). T cell–depleted bone marrow cells from $CD90.1^+$ or $CD45.1^+CD45.2^+$ wild-type donor (competitor) mice were mixed at a 1:1 ratio with $CD90.2^+CD45.2^+$ donor bone marrow cells (from wild-type, $DGK\zeta^{-/-}$, $CD28^{-/-}$, $DGK\zeta^{-/-}CD28^{-/-}$, c-$Rel^{-/-}$, c-$Rel^{+/-}$, $DGK\zeta^{-/-}$c-$Rel^{-/-}$, or $DGK\zeta^{-/-}$c-$Rel^{+/-}$ mice) and a total of 3 to 4×10^6 bone marrow cells were injected intravenously (i.v.) into lethally irradiated (11 Gy) $CD45.1^+$ recipient mice. The spleens and thymi of the mixed bone marrow chimeric mice were analyzed by flow cytometry 9 to 11 weeks after the bone marrow transplant. The percentage of nTreg cells ($Foxp3^+CD4^+$ cells as a percentage of all CD4 SP thymocytes) and the percentage of nTreg cell precursors ($CD25^+Foxp3^-CD4^+$ cells as a percentage of all CD4 SP thymocytes) of the experimental group ($CD90.2^+CD45.2^+$) and of the wild-type competitor ($CD90.1^+$ or $CD45.1^+CD45.2^+$) were determined for each mouse.

Western blotting analysis

MACS-sorted $CD4^+$ T cells from freshly isolated splenocytes were rested in serum-free RPMI for 2 hours. Alternatively, FACS-sorted $CD4^+Foxp3^-CD44^{lo}$ T cells were rested in T cell medium for 12 to 15 hours. Rested cells were incubated with biotinylated anti-CD3, anti-CD4, and anti-CD28 antibodies (all at 5 μg/ml) for 1 min in a 37°C water bath. Soluble streptavidin (25 μg/ml) was added immediately to crosslink the biotinylated antibodies for the times indicated in the figure legends. Stimulations were quenched by the addition of 1 ml of ice-cold PBS, followed by immediate lysis, as previously described (68). For inhibition of MEK1/2, cells were pretreated for one hour at 37°C with U0126 at various concentrations or with DMSO as a control, which was maintained throughout the assay. In some experiments, nuclear fractions were purified with NE-PER Nuclear and Cytoplasmic Extraction Reagents (Thermo Scientific) according to the manufacturer's directions. The lysates were resolved by SDS polyacrylamide gel electrophoresis (SDS-PAGE, Bio-Rad), and transferred to nitrocellulose membranes (Bio-Rad). The membranes were blocked for 1 hour with blocking reagent (Roche) and incubated with the appropriate primary antibody overnight at 4°C on a cell shaker. HRP-conjugated secondary antibodies (Bio-Rad) were used in combination with ECL reagents (GE Healthcare) to visualize the Western blots. The intensities of bands corresponding to total PLC-γ1 and pIκBα were quantified in Photoshop (Adobe Systems) by multiplying mean pixel intensity by the number of pixels within each band and subtracting the background intensity. The intensities of bands corresponding to pIκBα were normalized to those corresponding to PLC-γ1 and the resulting values were then divided by the normalized intensity of bands corresponding to pIκBα from WT T cells. Total ERK and pERK proteins were quantified with fluorescent secondary antibodies and the Odyssey imager and LI-COR imaging software (LI-COR Biosciences). The fluorescence intensity of the pERK band was divided by that of the total ERK band for each condition for normalization to the loading control. Each of the normalized pERK band intensities was divided by the normalized band intensity of pERK from WT T cells (DMSO control) to obtain relative pERK intensities. The relative pERK intensities were then plotted against the percentages of Treg cells obtained at each concentration of U0126. Linear regression analysis was performed on the linear portion of the curve with Prism software (GraphPad).

Statistical analyses

All values were graphed and analyzed for statistical significance with Prism software. Paired or unpaired two-tailed Student's t-tests were used to calculate each *P* value as indicated in the legends. *P* values < 0.05 were considered statistically significant.

Supplementary Material

Refer to Web version on PubMed Central for supplementary material.

Acknowledgments

We thank G. Koretzky and X. P. Zhong for the $DGK\zeta^{-/-}$ mice, H.-C. Liou for the $c\text{-}Rel^{-/-}$ mice, S. Hedrick for information regarding the ERK^{SEM} mice, and E. Behrens for providing key reagents. We thank M. May and K. McCorkell for valuable experimental advice, and members of the laboratories of T. Kambayashi, E. Behrens, K. Nichols, and G. Koretzky for helpful discussions. We thank J. Stadanlick for critical reading of the manuscript.
Funding: This work was supported by grants from the National Blood Foundation, the University of Pennsylvania

internal funds, the American Heart Association, the National Institutes of Health (R01HL111501 and R01HL107589), and the Intramural Research Program of the CCR/NCI/NIH.

References and Notes

1. Josefowicz SZ, Lu LF, Rudensky AY. Regulatory T cells: mechanisms of differentiation and function. Annu Rev Immunol. 2012; 30:531–564. [PubMed: 22224781]
2. Sakaguchi S, Yamaguchi T, Nomura T, Ono M. Regulatory T cells and immune tolerance. Cell. 2008; 133:775–787. [PubMed: 18510923]
3. Bennett CL, Christie J, Ramsdell F, Brunkow ME, Ferguson PJ, Whitesell L, Kelly TE, Saulsbury FT, Chance PF, Ochs HD. The immune dysregulation, polyendocrinopathy, enteropathy, X-linked syndrome (IPEX) is caused by mutations of FOXP3. Nat Genet. 2001; 27:20–21. [PubMed: 11137993]
4. Brunkow ME, Jeffery EW, Hjerrild KA, Paeper B, Clark LB, Yasayko SA, Wilkinson JE, Galas D, Ziegler SF, Ramsdell F. Disruption of a new forkhead/winged-helix protein, scurfin, results in the fatal lymphoproliferative disorder of the scurfy mouse. Nat Genet. 2001; 27:68–73. [PubMed: 11138001]
5. Kim JM, Rasmussen JP, Rudensky AY. Regulatory T cells prevent catastrophic autoimmunity throughout the lifespan of mice. Nat Immunol. 2007; 8:191–197. [PubMed: 17136045]
6. Lahl K, Loddenkemper C, Drouin C, Freyer J, Arnason J, Eberl G, Hamann A, Wagner H, Huehn J, Sparwasser T. Selective depletion of Foxp3+ regulatory T cells induces a scurfy-like disease. J Exp Med. 2007; 204:57–63. [PubMed: 17200412]
7. Sakaguchi S, Sakaguchi N, Asano M, Itoh M, Toda M. Immunologic self-tolerance maintained by activated T cells expressing IL-2 receptor alpha-chains (CD25). Breakdown of a single mechanism of self-tolerance causes various autoimmune diseases. J Immunol. 1995:1151–1164. [PubMed: 7636184]
8. Wang HY, Wang RF. Regulatory T cells and cancer. Curr Opin Immunol. 2007; 19:217–223. [PubMed: 17306521]
9. Belkaid Y, Rouse BT. Natural regulatory T cells in infectious disease. Nat Immunol. 2005; 6:353–360. [PubMed: 15785761]
10. Rowe JH, Ertelt JM, Way SS. Foxp3(+) regulatory T cells, immune stimulation and host defence against infection. Immunology. 2012; 136:1–10. [PubMed: 22211994]
11. Cebula A, Seweryn M, Rempala GA, Pabla SS, McIndoe RA, Denning TL, Bry L, Kraj P, Kisielow P, Ignatowicz L. Thymus-derived regulatory T cells contribute to tolerance to commensal microbiota. Nature. 2013
12. Singh B, Read S, Asseman C, Malmstrom V, Mottet C, Stephens LA, Stepankova R, Tlaskalova H, Powrie F. Control of intestinal inflammation by regulatory T cells. Immunol Rev. 2001; 182:190–200. [PubMed: 11722634]
13. Bilate AM, Lafaille JJ. Induced CD4+Foxp3+ regulatory T cells in immune tolerance. Annu Rev Immunol. 2012; 30:733–758. [PubMed: 22224762]
14. Lio CW, Hsieh CS. Becoming self-aware: the thymic education of regulatory T cells. Curr Opin Immunol. 2011; 23:213–219. [PubMed: 21146972]
15. Moran AE, Hogquist KA. T-cell receptor affinity in thymic development. Immunology. 2012; 135:261–267. [PubMed: 22182461]
16. Apostolou I, Sarukhan A, Klein L, von Boehmer H. Origin of regulatory T cells with known specificity for antigen. Nat Immunol. 2002; 3:756–763. [PubMed: 12089509]
17. Knoechel B, Lohr J, Kahn E, Bluestone JA, Abbas AK. Sequential development of interleukin 2-dependent effector and regulatory T cells in response to endogenous systemic antigen. J Exp Med. 2005; 202:1375–1386. [PubMed: 16287710]
18. Walker LS, Chodos A, Eggena M, Dooms H, Abbas AK. Antigen-dependent proliferation of CD4+ CD25+ regulatory T cells in vivo. J Exp Med. 2003; 198:249–258. [PubMed: 12874258]
19. Jordan MS, Boesteanu A, Reed AJ, Petrone AL, Holenbeck AE, Lerman MA, Naji A, Caton AJ. Thymic selection of CD4+CD25+ regulatory T cells induced by an agonist self-peptide. Nat Immunol. 2001:301–306. [PubMed: 11276200]

20. Kawahata K, Misaki Y, Yamauchi M, Tsunekawa S, Setoguchi K, Miyazaki J, Yamamoto K. Generation of CD4(+)CD25(+) regulatory T cells from autoreactive T cells simultaneously with their negative selection in the thymus and from nonautoreactive T cells by endogenous TCR expression. J Immunol. 2002:4399–4405. [PubMed: 11970982]
21. Lee HM, Bautista JL, Scott-Browne J, Mohan JF, Hsieh CS. A broad range of self-reactivity drives thymic regulatory T cell selection to limit responses to self. Immunity. 2012; 37:475–486. [PubMed: 22921379]
22. Kane LP, Lin J, Weiss A. Signal transduction by the TCR for antigen. Curr Opin Immunol. 2000; 12:242–249. [PubMed: 10781399]
23. Smith-Garvin JE, Koretzky GA, Jordan MS. T cell activation. Annu Rev Immunol. 2009; 27:591–619. [PubMed: 19132916]
24. Zhong XP, Hainey EA, Olenchock BA, Jordan MS, Maltzman JS, Nichols KE, Shen H, Koretzky GA. Enhanced T cell responses due to diacylglycerol kinase zeta deficiency. Nat Immunol. 2003; 4:882–890. [PubMed: 12883552]
25. Zhong XP, Hainey EA, Olenchock BA, Zhao H, Topham MK, Koretzky GA. Regulation of T cell receptor-induced activation of the Ras-ERK pathway by diacylglycerol kinase zeta. J Biol Chem. 2002; 277:31089–31098. [PubMed: 12070163]
26. Olenchock BA, Guo R, Carpenter JH, Jordan M, Topham MK, Koretzky GA, Zhong XP. Disruption of diacylglycerol metabolism impairs the induction of T cell anergy. Nat Immunol. 2006; 7:1174–1181. [PubMed: 17028587]
27. Joshi RP, Schmidt AM, Das J, Pytel D, Riese MJ, Lester M, Diehl JA, Behrens EM, Kambayashi T, Koretzky GA. The ζ isoform of diacylglycerol kinase plays a predominant role in regulatory T cell development and TCR-mediated Ras signaling. Sci. Signal. 2013; 6
28. Moran AE, Holzapfel KL, Xing Y, Cunningham NR, Maltzman JS, Punt J, Hogquist KA. T cell receptor signal strength in Treg and iNKT cell development demonstrated by a novel fluorescent reporter mouse. J Exp Med. 2011; 208:1279–1289. [PubMed: 21606508]
29. Osborne BA, Smith SW, Liu ZG, McLaughlin KA, Grimm L, Schwartz LM. Identification of genes induced during apoptosis in T lymphocytes. Immunol Rev. 1994; 142:301–320. [PubMed: 7698798]
30. Baldwin TA, Hogquist KA. Transcriptional analysis of clonal deletion in vivo. J Immunol. 2007; 179:837–844. [PubMed: 17617574]
31. Lio CW, Hsieh CS. A two-step process for thymic regulatory T cell development. Immunity. 2008; 28:100–111. [PubMed: 18199417]
32. Kishimoto H, Sprent J. Negative selection in the thymus includes semimature T cells. J Exp Med. 1997; 185:263–271. [PubMed: 9016875]
33. Burchill MA, Yang J, Vang KB, Farrar MA. Interleukin-2 receptor signaling in regulatory T cell development and homeostasis. Immunol Lett. 2007; 114:1–8. [PubMed: 17936914]
34. Wirnsberger G, Mair F, Klein L. Regulatory T cell differentiation of thymocytes does not require a dedicated antigen-presenting cell but is under T cell-intrinsic developmental control. Proc Natl Acad Sci U S A. 2009; 106:10278–10283. [PubMed: 19515822]
35. Vang KB, Yang J, Pagan AJ, Li LX, Wang J, Green JM, Beg AA, Farrar MA. Cutting edge: CD28 and c-Rel-dependent pathways initiate regulatory T cell development. J Immunol. 2011; 184:4074–4077. [PubMed: 20228198]
36. Burchill MA, Yang J, Vang KB, Moon JJ, Chu HH, Lio CW, Vegoe AL, Hsieh CS, Jenkins MK, Farrar MA. Linked T cell receptor and cytokine signaling govern the development of the regulatory T cell repertoire. Immunity. 2008; 28:112–121. [PubMed: 18199418]
37. Tai X, Cowan M, Feigenbaum L, Singer A. CD28 costimulation of developing thymocytes induces Foxp3 expression and regulatory T cell differentiation independently of interleukin 2. Nat Immunol. 2005; 6:152–162. [PubMed: 15640801]
38. Tuosto L. NF-kappaB family of transcription factors: biochemical players of CD28 co-stimulation. Immunol Lett. 2011; 135:1–9. [PubMed: 20863851]
39. Deenick EK, Elford AR, Pellegrini M, Hall H, Mak TW, Ohashi PS. c-Rel but not NF-kappaB1 is important for T regulatory cell development. Eur J Immunol. 2010; 40:677–681. [PubMed: 20082358]

40. Grigoriadis G, Vasanthakumar A, Banerjee A, Grumont R, Overall S, Gleeson P, Shannon F, Gerondakis S. c-Rel controls multiple discrete steps in the thymic development of Foxp3+ CD4 regulatory T cells. PLoS One. 2011; 6:e26851. [PubMed: 22066012]
41. Isomura I, Palmer S, Grumont RJ, Bunting K, Hoyne G, Wilkinson N, Banerjee A, Proietto A, Gugasyan R, Wu L, McNally A, Steptoe RJ, Thomas R, Shannon MF, Gerondakis S. c-Rel is required for the development of thymic Foxp3+ CD4 regulatory T cells. J Exp Med. 2009; 206:3001–3014. [PubMed: 19995950]
42. Long M, Park SG, Strickland I, Hayden MS, Ghosh S. Nuclear factor-kappaB modulates regulatory T cell development by directly regulating expression of Foxp3 transcription factor. Immunity. 2009; 31:921–931. [PubMed: 20064449]
43. Ruan Q, Kameswaran V, Tone Y, Li L, Liou HC, Greene MI, Tone M, Chen YH. Development of Foxp3(+) regulatory t cells is driven by the c-Rel enhanceosome. Immunity. 2009; 31:932–940. [PubMed: 20064450]
44. Zheng Y, Josefowicz S, Chaudhry A, Peng XP, Forbush K, Rudensky AY. Role of conserved non-coding DNA elements in the Foxp3 gene in regulatory T-cell fate. Nature. 2010; 463:808–812. [PubMed: 20072126]
45. Cheng J, Montecalvo A, Kane LP. Regulation of NF-kappaB induction by TCR/CD28. Immunol Res. 2011; 50:113–117. [PubMed: 21717079]
46. Brose N, Rosenmund C. Move over protein kinase C, you've got company: alternative cellular effectors of diacylglycerol and phorbol esters. J Cell Sci. 2002; 115:4399–4411. [PubMed: 12414987]
47. Favata MF, Horiuchi KY, Manos EJ, Daulerio AJ, Stradley DA, Feeser WS, Van Dyk DE, Pitts WJ, Earl RA, Hobbs F, Copeland RA, Magolda RL, Scherle PA, Trzaskos JM. Identification of a novel inhibitor of mitogen-activated protein kinase kinase. J Biol Chem. 1998; 273:18623–18632. [PubMed: 9660836]
48. Malek TR, Castro I. Interleukin-2 receptor signaling: at the interface between tolerance and immunity. Immunity. 2010; 33:153–165. [PubMed: 20732639]
49. Sharp LL, Schwarz DA, Bott CM, Marshall CJ, Hedrick SM. The influence of the MAPK pathway on T cell lineage commitment. Immunity. 1997; 7:609–618. [PubMed: 9390685]
50. Fontenot JD, Dooley JL, Farr AG, Rudensky AY. Developmental regulation of Foxp3 expression during ontogeny. J Exp Med. 2005; 202:901–906. [PubMed: 16203863]
51. Kim HP, Leonard WJ. The basis for TCR-mediated regulation of the IL-2 receptor alpha chain gene: role of widely separated regulatory elements. EMBO J. 2002; 21:3051–3059. [PubMed: 12065418]
52. Tan TH, Huang GP, Sica A, Ghosh P, Young HA, Longo DL, Rice NR. Kappa B site-dependent activation of the interleukin-2 receptor alpha-chain gene promoter by human c-Rel. Mol Cell Biol. 1992; 12:4067–4075. [PubMed: 1508203]
53. Kim HP, Imbert J, Leonard WJ. Both integrated and differential regulation of components of the IL-2/IL-2 receptor system. Cytokine Growth Factor Rev. 2006; 17:349–366. [PubMed: 16911870]
54. John S, Reeves RB, Lin JX, Child R, Leiden JM, Thompson CB, Leonard WJ. Regulation of cell-type-specific interleukin-2 receptor alpha-chain gene expression: potential role of physical interactions between Elf-1, HMG-I(Y), and NF-kappa B family proteins. Mol Cell Biol. 1995; 15:1786–1796. [PubMed: 7862168]
55. Mantel PY, Ouaked N, Ruckert B, Karagiannidis C, Welz R, Blaser K, Schmidt-Weber CB. Molecular mechanisms underlying FOXP3 induction in human T cells. J Immunol. 2006; 176:3593–3602. [PubMed: 16517728]
56. Yoshimi M, Goyama S, Kawazu M, Nakagawa M, Ichikawa M, Imai Y, Kumano K, Asai T, Mulloy JC, Kraft AS, Takahashi T, Shirafuji N, Kurokawa M. Multiple phosphorylation sites are important for RUNX1 activity in early hematopoiesis and T-cell differentiation. Eur J Immunol. 2012; 42:1044–1050. [PubMed: 22531928]
57. Tanaka T, Kurokawa M, Ueki K, Tanaka K, Imai Y, Mitani K, Okazaki K, Sagata N, Yazaki Y, Shibata Y, Kadowaki T, Hirai H. The extracellular signal-regulated kinase pathway phosphorylates AML1, an acute myeloid leukemia gene product, and potentially regulates its transactivation ability. Mol Cell Biol. 1996; 16:3967–3979. [PubMed: 8668214]

58. Ono M, Yaguchi H, Ohkura N, Kitabayashi I, Nagamura Y, Nomura T, Miyachi Y, Tsukada T, Sakaguchi S. Foxp3 controls regulatory T-cell function by interacting with AML1/Runx1. Nature. 2007; 446:685–689. [PubMed: 17377532]
59. Rudra D, Egawa T, Chong MM, Treuting P, Littman DR, Rudensky AY. Runx-CBFbeta complexes control expression of the transcription factor Foxp3 in regulatory T cells. Nat Immunol. 2009; 10:1170–1177. [PubMed: 19767756]
60. Gorentla BK, Wan CK, Zhong XP. Negative regulation of mTOR activation by diacylglycerol kinases. Blood. 2011; 117:4022–4031. [PubMed: 21310925]
61. Sauer S, Bruno L, Hertweck A, Finlay D, Leleu M, Spivakov M, Knight ZA, Cobb BS, Cantrell D, O'Connor E, Shokat KM, Fisher AG, Merkenschlager M. T cell receptor signaling controls Foxp3 expression via PI3K, Akt, and mTOR. Proc Natl Acad Sci U S A. 2008; 105:7797–7802. [PubMed: 18509048]
62. Haxhinasto S, Mathis D, Benoist C. The AKT-mTOR axis regulates de novo differentiation of CD4+Foxp3+ cells. J Exp Med. 2008; 205:565–574. [PubMed: 18283119]
63. Zhong XP, Guo R, Zhou H, Liu C, Wan CK. Diacylglycerol kinases in immune cell function and self-tolerance. Immunol Rev. 2008; 224:249–264. [PubMed: 18759932]
64. Tuosto L, Michel F, Acuto O. p95vav associates with tyrosine-phosphorylated SLP-76 in antigen-stimulated T cells. J Exp Med. 1996; 184:1161–1166. [PubMed: 9064333]
65. Yokosuka T, Kobayashi W, Sakata-Sogawa K, Takamatsu M, Hashimoto-Tane A, Dustin ML, Tokunaga M, Saito T. Spatiotemporal regulation of T cell costimulation by TCR-CD28 microclusters and protein kinase C theta translocation. Immunity. 2008; 29:589–601. [PubMed: 18848472]
66. Diaz-Flores E, Siliceo M, Martinez AC, Merida I. Membrane translocation of protein kinase Ctheta during T lymphocyte activation requires phospholipase C-gamma-generated diacylglycerol. J Biol Chem. 2003; 278:29208–29215. [PubMed: 12738795]
67. Liou HC, Jin Z, Tumang J, Andjelic S, Smith KA, Liou ML. c-Rel is crucial for lymphocyte proliferation but dispensable for T cell effector function. Int Immunol. 1999; 11:361–371. [PubMed: 10221648]
68. Kambayashi T, Okumura M, Baker RG, Hsu CJ, Baumgart T, Zhang W, Koretzky GA. Independent and cooperative roles of adaptor molecules in proximal signaling during FcepsilonRI-mediated mast cell activation. Mol Cell Biol. 2010; 30:4188–4196. [PubMed: 20606011]

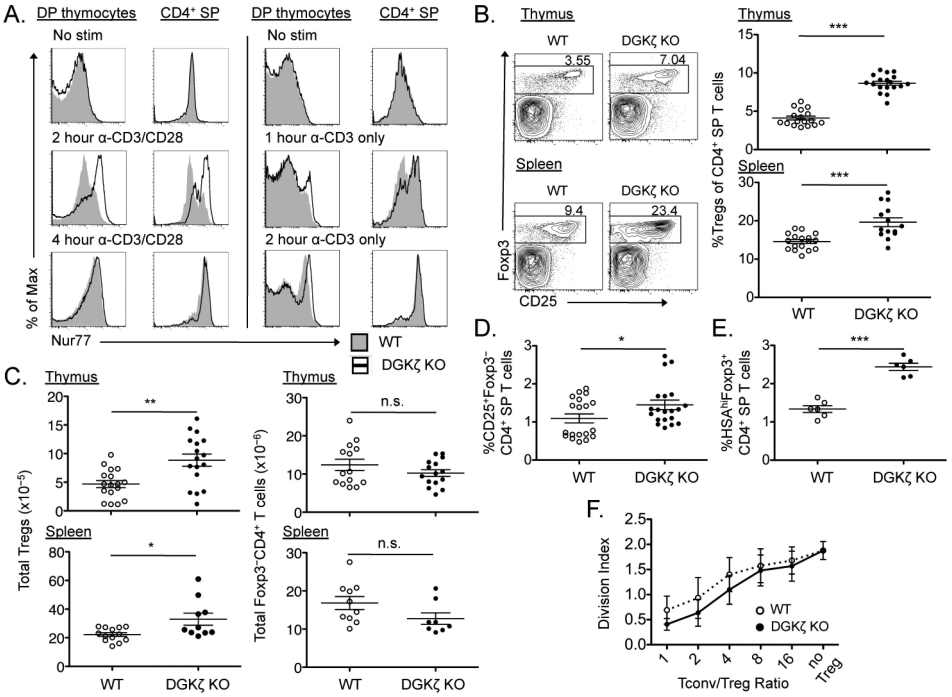

Fig. 1. DGKζ$^{-/-}$ mice exhibit increased percentages of thymic and peripheral Treg cells

(**A**) Freshly isolated thymocytes from wild-type (WT) and DGKζ$^{-/-}$ [DGKζ knockout (KO)] mice were stimulated with anti-CD3 antibody alone or in the presence of anti-CD28 antibody for the indicated times, and then were analyzed by flow cytometry to assess Nur77 abundance in DP thymocytes and CD4 SP thymocytes. Plots show intracellular staining for Nur77 in WT (shaded histogram) and DGKζ$^{-/-}$ (open histogram) thymocytes from one experiment, and are representative of three independent experiments. (**B** and **C**) The thymi (top) and spleens (bottom) of WT (open circles) and DGKζ$^{-/-}$ (closed circles) mice were analyzed by flow cytometry to detect Foxp3 and CD25. Representative flow cytometric profiles (gated on CD4$^+$ live singlets) and scatter plots with means ± SEM of (B) the percentages of Treg cells within live CD4 SP T cells and (C) the absolute numbers of Treg cells (left) and Foxp3$^-$CD4$^+$ T cells (right) from five compiled experiments are shown, with each circle representative of a single mouse. (**D**) Scatter plots showing means ± SEM of the percentages of CD25$^+$Foxp3$^-$CD4$^+$ Treg cell precursors within the population of live CD4 SP T cells in the thymi of the indicated mice. Data from five compiled experiments are shown, with each circle representative of a single mouse. (**E**) Scatter plots showing means ± SEM of the percentages of HSA^{hi}Foxp3$^+$CD4$^+$ T cells in the thymi of the indicated mice. Data from two compiled experiments are shown, with each circle representative of a single mouse. (**F**) CFSE-labeled, FACS-sorted splenic Foxp3$^-$CD4$^+$ T cells (conventional T cells, Tconv) were co-cultured with FACS-sorted WT or DGKζ$^{-/-}$ Treg cells at various ratios of Tconv:Treg for four days in the presence of irradiated, T cell–depleted splenocytes and anti-CD3 antibody. The division index of Tconvs is represented as the mean ± SEM of three independent experiments. *P < 0.05, **P < 0.01, and ***P < 0.001, by unpaired two-tailed student's t-test. n.s., not significant.

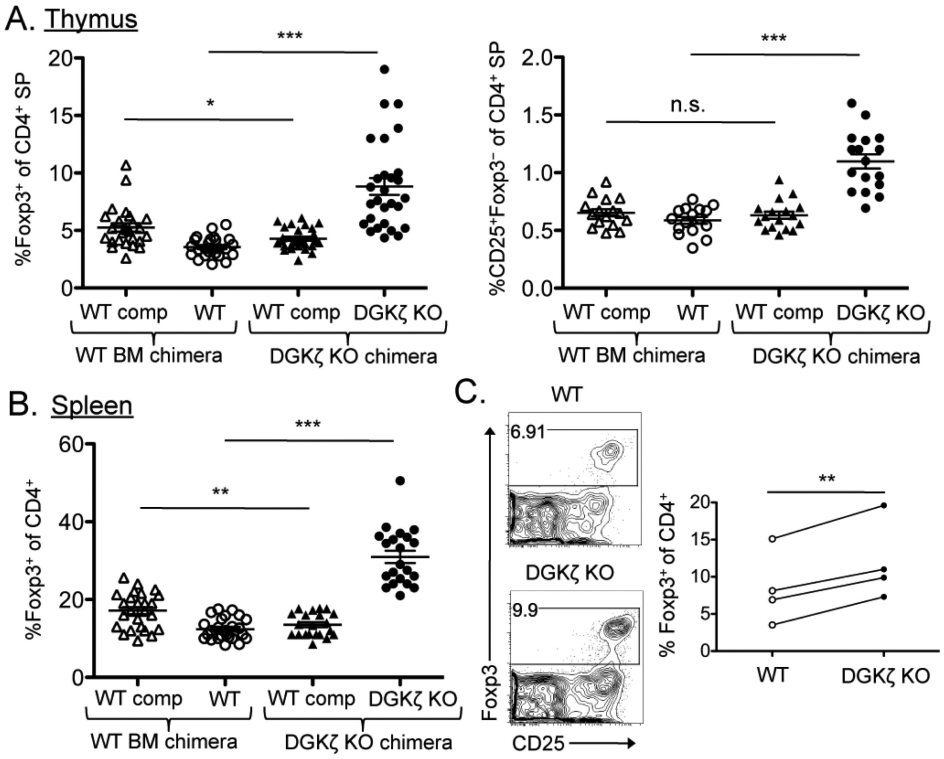

Fig. 2. The enhanced generation of nTreg cells in DGKζ$^{-/-}$ mice is cell-intrinsic

(**A** and **B**) Mixed bone marrow chimeric mice were generated by reconstitution of lethally irradiated recipient mice with a 1:1 ratio of WT or DGKζ$^{-/-}$ bone marrow cells with congenically disparate WT competitor bone marrow cells, and were analyzed 9 to 11 weeks after transplant by flow cytometry. Scatter plots show means ± SEM of (A) the percentages of Foxp3^{+}CD4^{+} Treg cells (left) and CD25^{+}Foxp3^{-}CD4^{+} cells (right) within the total population of CD4 SP thymocytes, and (B) the percentages of Foxp3^{+}CD4^{+} Treg cells within the total population of CD4^{+} T cells within the experimental (CD45.2^{+}) or the WT competitor fraction (CD45.1^{+}). Data from six compiled experiments are shown, with each symbol representative of a single chimera. (**C**) Immature CD4 SP thymocytes (Foxp3^{-}CD25^{-}CD44^{lo}CD69^{hi}) were sorted from the thymi of WT and DGKζ$^{-/-}$ Foxp3.GFP reporter mice and were cultured in the presence of IL-2 and anti-CD3 antibody. Foxp3 abundance was assessed 72 hours later by flow cytometry. Left: Flow cytometric profiles showing Foxp3 and CD25 staining in cells that were previously gated on CD4^{+} live singlets. Plots are from a single experiment and are representative of four independent experiments. Right: Compiled data from four independent experiments showing the percentages of CD4 SP cells that are Foxp3^{+}. *P < 0.05, **P < 0.01, and ***P < 0.001, by unpaired [for (A) and (B)] or paired [for (C)] two-tailed student's t-test.

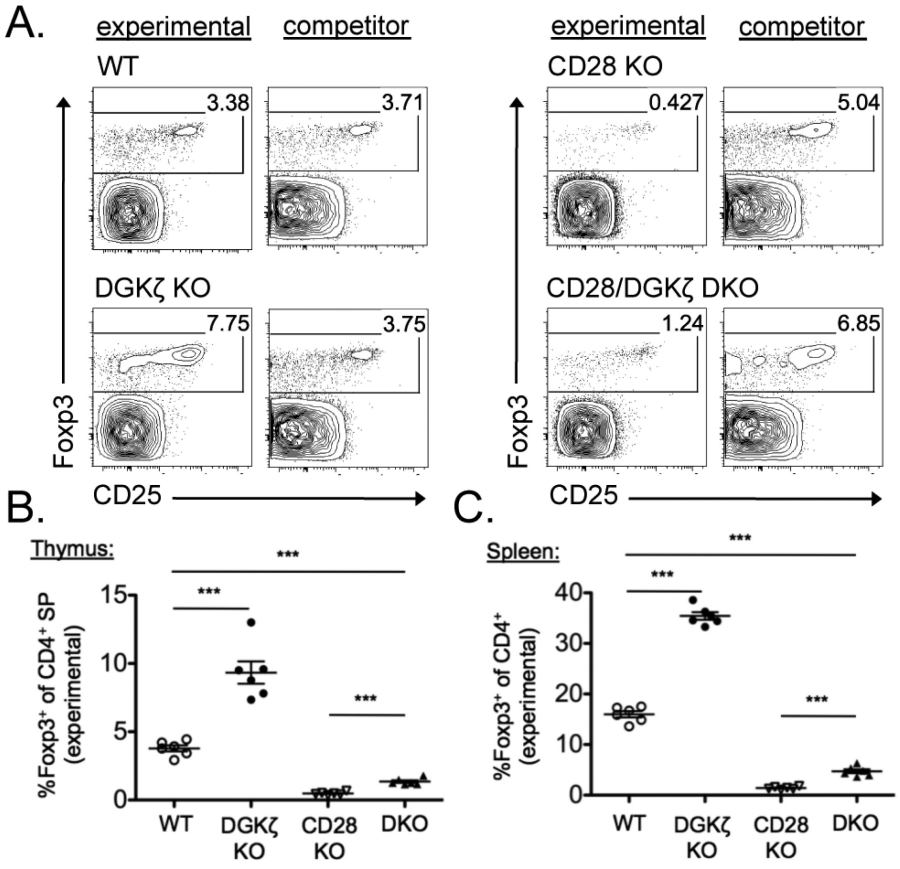

Fig. 3. Loss of DGKζ cannot rescue the developmental defect in Treg cells intrinsic to CD28$^{-/-}$ mice

(**A** to **C**) Mixed bone marrow chimeric mice were generated by reconstitution of lethally irradiated recipient mice with a 1:1 ratio of WT, DGKζ$^{-/-}$, CD28$^{-/-}$, or DGKζ$^{-/-}$CD28$^{-/-}$ bone marrow cells with congenically disparate WT competitor bone marrow cells, and were analyzed 9 to 11 weeks later by flow cytometry. Flow cytometric profiles of cells from the thymi of the indicated mice, gated on experimental (CD45.2^{+}) or competitor (CD45.1) CD4^{+} live singlets, are shown and are representative of six individual chimeric mice per group. Scatter plots show means ± SEM of the percentages of total CD4 SP T cells that are Foxp3^{+}CD4^{+} Treg cells within the experimental fraction in (B) the thymus and (C) the spleen. Data are compiled from one experiment, with each symbol representative of a single chimeric mouse. *** $P < 0.001$ by unpaired two-tailed student's t-test.

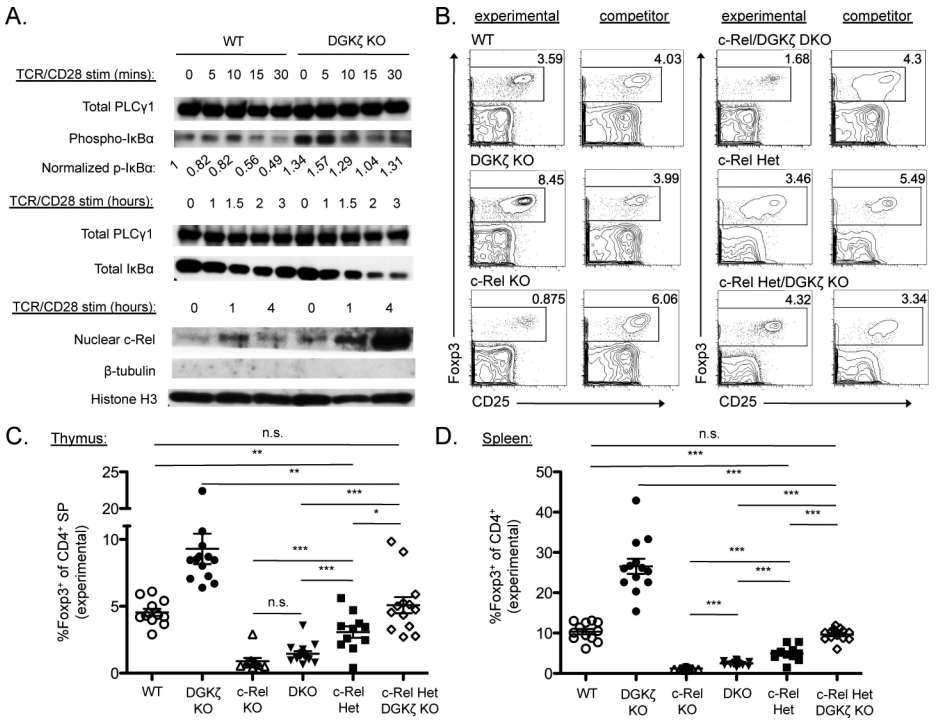

Fig. 4. c-Rel signaling is augmented in DGKζ$^{-/-}$ T cells and is required for the enhanced development of Treg cells in DGKζ$^{-/-}$ mice

(**A**) MACS-sorted CD4$^+$ T cells (for the analysis of IκBα) or FACS-sorted Foxp3$^-$CD44^{lo}CD4$^+$ T cells (for the analysis of c-Rel) from the spleens of WT and DGKζ$^{-/-}$ mice were stimulated through the TCR and CD28 for the indicated times. Total cell lysates were analyzed by Western blotting to detect the phosphorylation (top) and degradation (middle) of IκBα. Total PLC-γ1 served as a loading control for these blots. PLC-γ1 and pIκBα band intensities were quantified with imaging software, pIκBα bands were normalized to the corresponding PLC-γ1 bands, and all values were then divided by the normalized pIκBα intensity calculated for unstimulated WT T cells. Nuclear extracts of the indicated cells were analyzed by Western blotting to detect c-Rel (bottom). Histone H3 was used as a nuclear protein loading control, whereas β-tubulin was used to assess cytoplasmic contamination. Western blots and quantifications shown are from a single experiment and are representative of at least three independent experiments. (**B**) Mixed bone marrow chimeric mice were generated with a 1:1 ratio of WT, DGKζ$^{-/-}$, c-Rel$^{-/-}$, DGKζ$^{-/-}$c-Rel$^{-/-}$, c-Rel$^{+/-}$, or DGKζ$^{-/-}$ c-Rel$^{+/-}$ mice with congenically disparate WT competitor bone marrow cells, and were analyzed 9 to 11 weeks later by flow cytometry. Flow cytometric profiles from the thymus, gated on experimental (CD45.2$^+$) or competitor (CD45.1$^+$/CD45.2$^+$) CD4$^+$ live singlets from a single experiment are shown and are representative of chimeras generated in three independent experiments. (**C** and **D**) Scatter plots show the mean ± SEM percentages of total CD4 SP T cells that are Foxp3$^+$CD4$^+$ Treg cells within the experimental fraction in (C) the thymus and (D) the spleen. Data are compiled from three experiments, with each symbol representative of a single chimeric mouse. *P < 0.05, **P < 0.01, and ***P < 0.001, by unpaired two-tailed student's t-test.

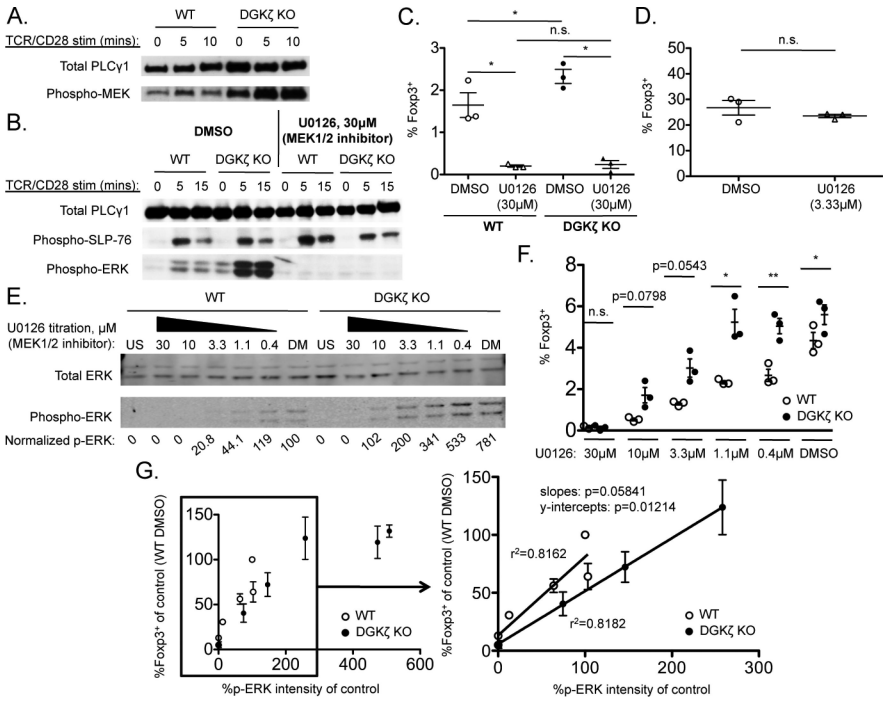

Fig. 5. ERK phosphorylation is required for the enhanced development of Treg cells in DGKζ$^{-/-}$ mice

(**A** and **B**) FACS-sorted Foxp3^{-}CD44^{lo}CD4^{+} T cells were pretreated with or without 30 μM U0126 for 1 hour and then were stimulated through the TCR and CD28 for the indicated times. Cell lysates were analyzed by Western blotting to detect the phosphorylation of (A) MEK or (B) SLP-76 and ERK. Total PLC-γ1 protein served as a loading control. Western blots are representative of three independent experiments. (**C**) FACS-sorted immature CD4 SP thymocytes (Foxp3^{-}CD25^{-}CD44^{lo}CD69^{hi}) from the thymi of WT or DGKζ$^{-/-}$ Foxp3.GFP reporter mice were pretreated with or without 30 μM U0126 for 1 hour and then were stimulated with IL-2 together with anti-CD3 and anti-CD28 antibodies in the presence of U0126 for 20 hours. Scatter plots shown the mean ± SEM of the percentages of CD4^{+} cells that were Foxp3^{+}. Data are from three independent experiments. (**D**) FACS-sorted immature CD4 SP thymocytes (Foxp3^{-}CD25^{-}CD44^{lo}CD69^{hi}) from the thymi of WT Foxp3.GFP reporter mice were stimulated with IL-2 for 20 hours. CD25^{+} cells were then FACS-sorted from these cultures, pretreated with or without 3.33 μM U0126 for 1 hour, and then were stimulated with IL-2 alone for an additional 60 hours. Scatter plots shown the mean ± SEM of the percentages of CD4^{+} cells that were Foxp3^{+}. Data are from three independent experiments. (**E**) FACS-sorted Foxp3^{-}CD44^{lo}CD4^{+} T cells were pretreated with or without the indicated concentrations of U0126 for 1 hour and then stimulated through their TCR in the presence of U0126 for 5 min. Cell lysates were analyzed by Western blotting with antibodies specific for total ERK and pERK, which were quantified by the Odyssey imaging system. The normalized values for pERK represent the intensities of the bands corresponding to pERK p42 divided by the intensities of the bands corresponding to total ERK (p42) and normalized to the value for the DMSO-treated WT CD4^{+} T cells (which was set at 100%). US, unstimulated; DM, DMSO-treated. Western blots and quantifications shown are from a single experiment and are representative of three

independent experiments. (**F**) FACS-sorted immature CD4 SP thymocytes from the thymi of WT or DGKζ$^{-/-}$ Foxp3.GFP reporter mice were pretreated with or without the indicated concentrations of U0126 for 1 hour, and then were stimulated with IL-2 and anti-CD3 antibody in the presence of U0126 for 72 hours. Scatter plot shows means ± SEM of the percentages of CD4^{+} cells that were Foxp3^{+} for each concentration of U0126, and are from three independent experiments. (**G**) Normalized pERK values obtained from three independent experiments were averaged and plotted against the fraction of CD4^{+} cells that were Foxp3^{+} (normalized to DMSO-treated WT immature thymocytes for each experiment from three independent experiments) at each concentration of U0126 for WT (open circles) and DGKζ$^{-/-}$ T cells (closed circles). Linear regression analysis was performed on the linear portion of the curve to assess the relationship between the extent of ERK phosphorylation and the percentage of Foxp3^{+} T cells for WT and DGKζ$^{-/-}$ T mice. *$P < 0.05$, **$P < 0.01$, by paired two-tailed student's t-test.

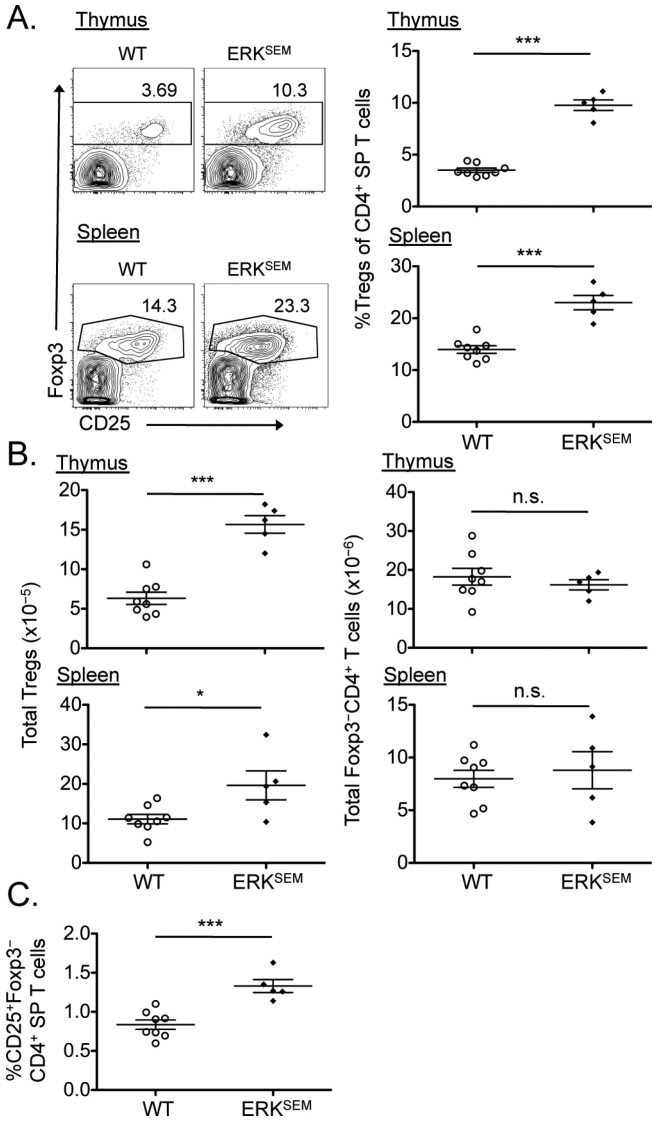

Fig. 6. Selective enhancement of ERK pathway activation leads to the increased development of Treg cells in vivo

(**A**) The thymi (top) and spleens (bottom) of WT (open circles) and ERK^{SEM} (closed diamonds) mice were analyzed by flow cytometry to detect Foxp3 and CD25. Left: Flow cytometric profiles (gated on CD4$^+$ live singlets) of Foxp3 and CD25 staining are representative of all mice within a single experiment. Right: Scatter plots show means ± SEM of the percentages of live CD4 SP T cells that were Treg cells for all mice compiled from one experiment, with each symbol representative of a single mouse. (**B**) Absolute numbers of Treg cells (left) and Foxp3$^-$CD4$^+$ T cells (right) in the thymi (top) and spleens (bottom) of the indicated mice from the experiments shown in (A). (**C**) Scatter plots show means ± SEM of the percentages of CD25$^+$Foxp3$^-$CD4$^+$ T cell precursors within the population of live CD4 SP T cells in thymus for all mice compiled from one experiment, with each symbol representative of a single mouse. *P < 0.05, ***P < 0.001, by unpaired two-tailed student's t-test.

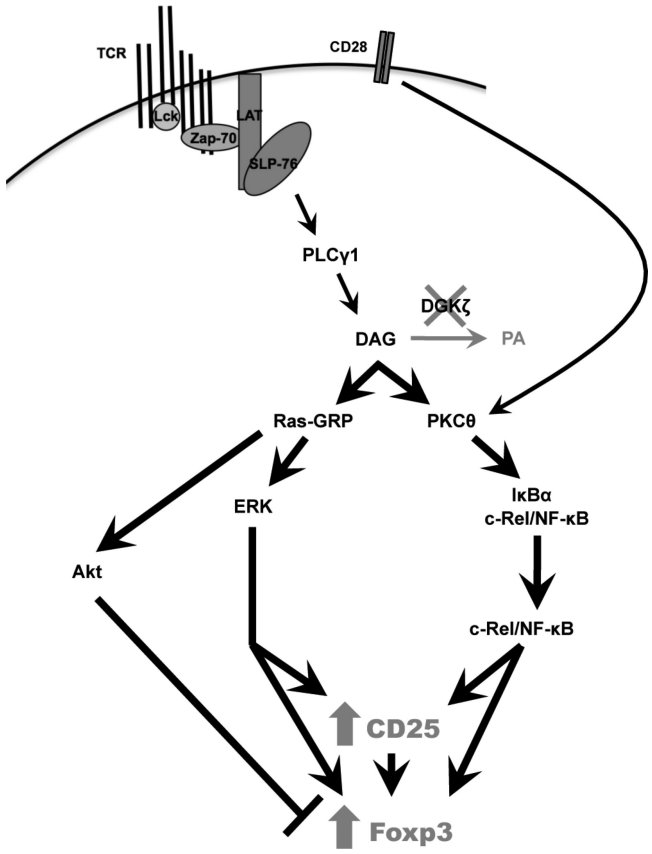

Fig. 7. DGKζ inhibits the expression of CD25 and Foxp3 in developing T cells

In the absence of DGKζ, intracellular DAG accumulates and leads to prolonged activation of Ras-GRP and PKCθ. Consequently, activation of the ERK and c-Rel pathways is enhanced, resulting in the increased cell-surface abundance of CD25 and induction of *Foxp3* expression in developing thymocytes. Prolonged DAG-mediated activation of PKCθ may mimic, but cannot replace, costimulation of CD28 by increasing the extent of c-Rel activation. The generation of Treg cells is partially countered by Akt-mediated signals that are simultaneously enhanced by the accumulation of DAG. Overall, there is a net gain in the extent of Treg cell generation in the context of DGKζ deficiency.